Journal of Alloys and Compounds xxx (2014) xxx–xxx

Contents lists available at ScienceDirect

Journal of Alloys and Compounds

journal homepage: www.elsevier.com/locate/jalcom

The structure of rapidly quenched Fe–Co–B–Si based systems and the influence of addition of Cu and P

I. Janotová *, P. Švec, I. Mat'ko, D. Janičkovič, P. Švec Sr.

Institute of Physics, Slovak Academy of Sciences, Dubravska cesta 9, 845 11 Bratislava, Slovakia

ARTICLE INFO

Article history:
Available online xxxx

Keywords:
Soft magnetic materials
Amorphous materials
Iron–boron alloys
Nanocrystalline structure

ABSTRACT

Rapidly quenched systems based on Fe–Co–B–Si with addition of Cu and P are very interesting for their excellent soft magnetic and mechanical properties. These physical properties are given by the structure formed from amorphous state after controlled annealing. Selected amorphous systems of this type have been prepared by planar flow casting in form of thin ribbons. Materials after heat treatment exhibit fine-grains of bcc-Fe in amorphous matrix and subsequently borides. The influence of the substitution of Fe for Co, the substitution of B for Si and the additions of P and Cu on structure in nanocrystalline state was investigated.

Transformations were detected using the methods of differential scanning calorimetry (DSC). X-ray diffraction (XRD), transmission electron microscopy (TEM) and electron diffraction (ED) analyses on samples heat-treated at selected temperatures were performed to obtain information about the structure, morphology, size and distribution of transformed grains in amorphous matrix of the investigated system.

1. Introduction

The effect of the addition of combinations of P, Si and Cu into metastable rapidly quenched Fe–Co–B alloys on formation of novel soft magnetic nanocrystalline materials with outstanding properties is in focus of recent investigations [1,2]. Such material systems are tailorable both by compositional optimization and by suitable thermal treatment and open new frontiers for enhancement of specific physical properties. Their structure consists of small bcc-Fe grains in amorphous matrix and exhibits high saturation magnetic flux density, high permeability and low magnetic loss. The additions of P and Si enhance stability of the bcc-Fe structure, the substitution of Fe for Co results generally in higher Curie temperature and in improvement of soft magnetic properties while Cu aids in refinement of the morphology of small ferromagnetic grains [1–8].

The addition of small amounts of metals like Cu into Fe–B based systems is known to enhance nucleation by forming energetically suitable sites for the formation of clusters. Our intention was to create a sufficiently stable nanocrystalline system by primary crystallization from as-cast rapidly quenched state, i.e. with stable bcc-Fe nano-phase in a wide temperature interval before the transformation of the amorphous remains takes place and which satisfies the requirements on the structurally-dependent magnetic properties. The goal of the highest content of ferromagnetic elements (which account for the ferromagnetic nature) with respect to metalloid elements in the alloys with maximalized content of nanograins in amorphous matrix leads to the necessity of optimization of nanocrystallization kinetics as well as to compositional optimization. The aim of the paper is to present temperature evolution of selected physical properties and of the structure of the studied systems.

Soft magnetic systems based on $(Fe_{85-x}Co_xB_{10}Si_5)_{100-y-z}P_yCu_z$, where $x = 0$; 21, $y = 0$; 3 and $z = 0$; 1 were prepared from rapidly quenched amorphous ribbons by regulated annealing.

2. Experimental procedure

Amorphous ribbons with thickness around 20 μm and width of 6 mm were prepared by planar flow casting (PFC) from master alloys with desired chemical composition (purity of the components was better than 99.9%). Casting of ribbons was performed after induction melting of the master alloys to casting temperatures about 200 K higher than the alloy melting point. The composition of the prepared samples is in Table 1. The amorphous state after rapid quenching was checked by X-ray diffraction analysis (XRD) in Bragg–Brentano geometry using Bruker D8 Advance diffractometer (Cr Kα radiation). The phase evolution during transformations stages was studied by means of in situ XRD during linear heating with the rate 5 K/min in in-house constructed hot chamber attachment of the diffractometer. The temperature was sensed and controlled with an *K*-type thermocouple that was embedded just beneath and touching a non-reflecting Si wafer. The thickness of the Si wafer was 0.4 mm. Temperature was calibrated by melting high purity standards, Sn and Al. The temperature controller used was a Eurotherm 2604 with auto-tuning option for setting the optimum PID parameters. Major construction elements of the furnace are low thermal expansion materials such as quartz. Thermomechanical behavior of the furnace and sample holder has been tested by linear heating and cooling scans with 5 K/min of a 20 μm thin Ni foil as sample. The thermal expansion of the fcc-Ni lattice has been determined as ~13.2 ± 0.3 ppm, close to the tabular value of ~16 ± 1 ppm in the temperature

* Corresponding author. Tel.: +421 903847077.
E-mail address: irena.janotova@savba.sk (I. Janotová).

0925-8388/$ - see front matter © 2013 Elsevier B.V. All rights reserved.
http://dx.doi.org/10.1016/j.jallcom.2013.12.044

Table 1
Results from thermal analysis (DSC and TGA): the temperature of the crystallizations onset T_x, the temperature of the maximum crystallizations rate T_{max}, the Curie temperature T_c of the as-quenched samples (indices 1 and 2 correspond to the first and second transformation, respectively).

	T_{x1} (K) ± 0.2	T_{max1} (K) ± 0.2	T_{x2} (K) ± 0.2	T_{max2} (K) ± 0.2	T_c (K) ± 0.5
$Fe_{85}B_{10}Si_5$	673.8	694.9	787.5	797.8	682.5
$(Fe_{85}B_{10}Si_5)_{99}Cu_1$	619.8	655.6	781.6	792.9	–
$(Fe_{85}B_{10}Si_5)_{97}P_3$	729.6	741.1	785.6	795.9	–
$(Fe_{85}B_{10}Si_5)_{96}P_3Cu_1$	780.2	784.0	–	806.9	–
$Fe_{64}Co_{21}B_{10}Si_5$	652.9	676.0	808.7	818.6	765[a]
$(Fe_{64}Co_{21}B_{10}Si_5)_{99}Cu_1$	650.7	670.2	800.1	809.6	790[a]
$(Fe_{64}Co_{21}B_{10}Si_5)_{97}P_3$	691.2	701.1	794.8	805.3	788[a]
$(Fe_{64}Co_{21}B_{10}Si_5)_{96}P_3Cu_1$	805.1	811.4	–	823.5	790[a]

[a] Estimate only, because $T_C > T_{X1}$.

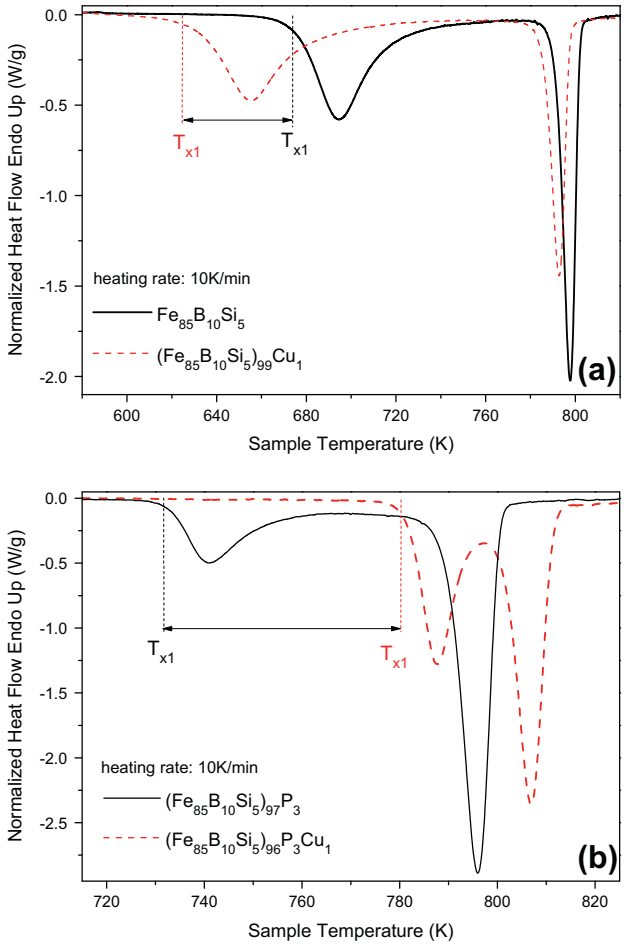

Fig. 1. DSC curves for samples based on $Fe_{85}B_{10}Si_5$ (a) with addition of 1at.% Cu and 3 at.% P (b).

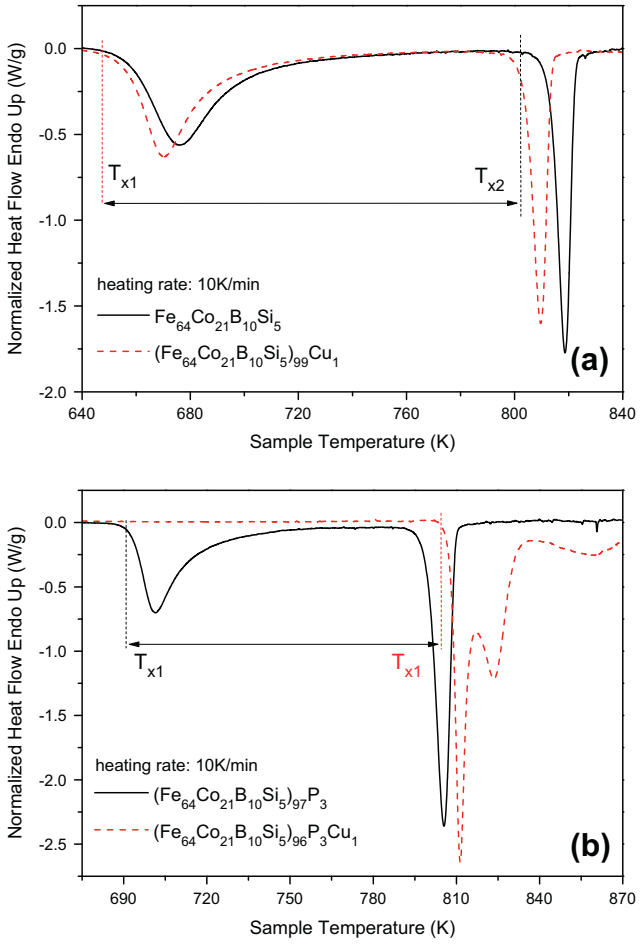

Fig. 2. DSC curves for samples based on $Fe_{64}Co_{21}B_{10}Si_5$ (a) with addition of 1at.% Cu and 3 at.% P (b).

range 350–950 K. The observed peaks were fitted by Bruker TOPAS v3. The morphology of the formed phases in samples after in situ XRD to selected temperatures was observed by transmission electron microscopy (TEM) using JEOL 2000FX at 200 kV. The kinetics of formation of crystalline phases was investigated by differential scanning calorimetry (DSC) using Perkin Elmer DSC 7 at heating rate 10 K/min in argon atmosphere. The different transformation stages were monitored also by magnetic thermogravimetry (TGA) using Perkin Elmer TGA 7 with small external magnet with the same heating rate in argon atmosphere in order to determine the temperature evolution of the ferromagnetic phases.

3. Results and discussion

The kinetics of investigated formations of crystalline phases from amorphous state was determined by DSC. These measurements show two individual, in temperature and time separated crystallization stages. Nanocrystallization, in first step of transformation of metallic glasses where bcc-Fe(Co) is formed, is characterized by no sharp onset. The slow onset (slope of DSC curve) of this transformation indicates long range diffusion-controlled primary crystallization. The entire process is a nucleation-and-growth Avrami-type transformation, very dissimilar to the grain growth kinetics observed in e.g. FINEMET-type alloys [9,10]. The second stage exhibits a sharp and often asymmetric onset of the DSC peak. The onset temperatures of the first (T_{x1}) and the second (T_{x2}) transformation stages are presented in Figs. 1 and 2, showing also the temperature interval between the values of T_{x1} for the samples without Cu and with Cu. This interval varies according to the elemental additions (and